AIAA JOURNAL
Vol. 47, No. 11, November 2009

Novel Technique for Measurements of Continuous Liquid Jet Core in an Atomizer

G. Charalampous,* Y. Hardalupas,† and A. M. K. P. Taylor‡
Imperial College London, London, England SW7 2BX, United Kingdom

DOI: 10.2514/1.40038

A novel optical method is proposed for the measurement of the length of the continuous liquid jet core in atomizers. Laser light is directed through the injecting nozzle to illuminate internally the liquid jet, which acts as an optical fiber transmitting the laser beam. The continuous core of the liquid jet is visualized by means of laser-induced fluorescence, generated by the addition of dye in the liquid. The instantaneous continuous length of the liquid jet is measured as the distance from the nozzle exit, where the emitted laser-induced fluorescence intensity from the liquid jet becomes negligibly small due to interruption of laser light transmission through the liquid jet following the liquid jet breakup. The method provides a nonintrusive measurement approach, promising improved measurements in dense sprays, where droplets obstruct the illumination and the imaging path of shadowgraphic techniques. Measurements in an air-blast atomizer showed that the continuous liquid length measured by the novel approach is systematically shorter than that measured by shadowgraphy. As such, existing empirical correlations for the breakup length, which have been mainly measured by shadowgraphy, may need to be revisited.

Nomenclature

D_G = inner diameter of the gaseous jet nozzle
D_L = inner diameter of liquid jet nozzle
D_0 = outer diameter of the liquid jet nozzle
L = breakup length
MR = gas to liquid momentum ratio
Re_L = liquid Reynolds number
U_G = cross section average gaseous velocity at the annulus
U_L = cross section average liquid velocity at the nozzle exit
We = Weber number at nozzle exit
ν_L = kinematic viscosity of the liquid
ρ_G = density of coaxial gas stream
ρ_L = density of central liquid jet
σ = surface tension

I. Introduction

THE process of coaxial air-blast atomization in combustion systems, such as rocket engines and gas turbines, is a complex phenomenon that has been investigated by many researchers, including [1–7]. Successful atomization of the liquid jet will provide sufficiently small droplet sizes, which can thoroughly evaporate and improve mixing between the liquid vapor and the surrounding gas, which is important for combustion applications.

The atomization process takes place in two regions, the primary and the secondary. In the primary breakup region, the shear forces at the gas–liquid interface are responsible for the breakup of the liquid jet into droplets and ligaments. The liquid jet usually remains continuous over several liquid jet diameters downstream of the nozzle exit depending on flow conditions, such as liquid and gas velocities, nozzle geometry, and the physical properties of the two fluids. Downstream of the primary breakup, the secondary atomization region follows, during which further atomization of droplets and ligaments occurs due to deformation by the surrounding gas stream [8].

The process of atomization itself can be characterized by a number of factors among which is the length of the continuous core of the liquid jet, which is also known as breakup length. The length of the continuous liquid jet core determines the extent of the primary atomization region and is very important for the performance of atomizing nozzles and for the development of computational models of the atomization process. However, it is usually difficult to probe into this region due to the formation of a dense cloud of droplets and ligaments around the central liquid jet. Currently, most methods used for the quantification of the continuous length are either intrusive [9,10] or photographic [6,11]. Both have limitations. The former method affects the atomization process due to the presence of a physical probe in the flow. In the latter, which is the most commonly used, the spray is illuminated by background lighting provided by a lamp or a laser, and shadowgraphs of the breakup region are recorded. However, the shadowgraphic images of the continuous liquid core are hindered by the presence of the products of atomization (ligaments and droplets), which can lead to erroneous measurements of the length of the continuous liquid jet core. Yet, most empirical correlations for the breakup length are based on shadowgraphic measurements, which generates doubts on their accuracy. More recent methods for investigating the structure of sprays that could be used to evaluate the continuous length of sprays are x-ray absorption [12–14], which is based on the measurement of the attenuation of x-ray beams passing through the investigated spray and ballistic imaging [15–17] where the investigated spray is back illuminated by a very short laser pulse (pulse duration on the order of femtosecond), and only the photons that pass through the spray without being scattered by the spray liquid are imaged. However, both these methods are very expensive to implement and require highly specialized equipment.

In this paper, we describe a novel optical technique for the measurement of the breakup length of liquid jets, which is based on the illumination of the liquid jet from within the injecting nozzle. In this case, the liquid jet acts as an optical fiber, with the propagation of light interrupted at the breakup region. A fluorescing dye added to the atomizing liquid is excited by the propagating laser beam and, as a result, the volume of the continuous portion of the liquid jet fluoresces. The novel technique was used to measure the breakup length of the liquid jet in a coaxial air-blast atomizer. The breakup length was also measured simultaneously by means of conventional shadowgraphy. Comparison is made between the two techniques and

Presented as Paper 1337 at the 45th AIAA Aerospace Sciences Meeting and Exhibit, Reno, NV, 8–11 January 2007; received 25 July 2008; revision received 15 May 2009; accepted for publication 7 July 2009.

*Research Assistant, Department of Mechanical Engineering; georgios.charalampous@imperial.ac.uk.

†Professor, Department of Mechanical Engineering; y.hardalupas@imperial.ac.uk. Associate Fellow AIAA.

‡Professor, Department of Mechanical Engineering; a.m.taylor@imperial.ac.uk.

the merits and limitations of the novel technique are indicated. The remaining paper is structured as follows. The next section describes the flow configuration and the experimental methods. Section III presents results for liquid jets in quiescent air and in coaxial airstreams, and discusses the advantages and limitations of the novel technique. Finally, it compares the breakup measurements with the novel technique and the shadowgraphic method. The paper ends with a summary of the main findings.

II. Flow Configuration and Experimental Methods

The experimental investigation was performed on the coaxial air-blast atomizer configuration, described in detail in [11]. In the current investigation, the atomizer was placed vertically and the spray exhausted downward. The external and internal diameter of the liquid nozzle was 2.95 and 2.3 mm, respectively, and the internal diameter of the coaxial air nozzle was 14.95 mm.

For the introduction of the laser beam through the atomizer liquid nozzle, the original configuration of the atomizer was modified as shown in Fig. 1. A hollow tube open at the top end and fitted with a quartz window at the lower end was inserted within the central tube of the atomizing liquid, up to the entrance of the conical contraction of the liquid nozzle. This addition acts as a light guide, which allows a laser pulse to propagate through the central tube without interacting with the liquid for the full length of the central tube. Upstream of the liquid nozzle exit, the laser beam exits through the light-guide tube window, propagates through the liquid and exits through the nozzle in the same direction as the flow of the atomizing liquid. In this way, the continuous liquid jet acts as an optical fiber (a phenomenon that has been demonstrated as early as the 19th century by Colladon [18] and Tyndall [19]), which allows the propagation of the laser light until the location of the breakup. Introducing the laser beam from within the liquid nozzle directly within the continuous section of the liquid jet is free of the attenuation that would otherwise be caused by introduction of the laser illumination through the surrounding spray and ensures that low light intensity is present beyond the surface of the liquid jet.

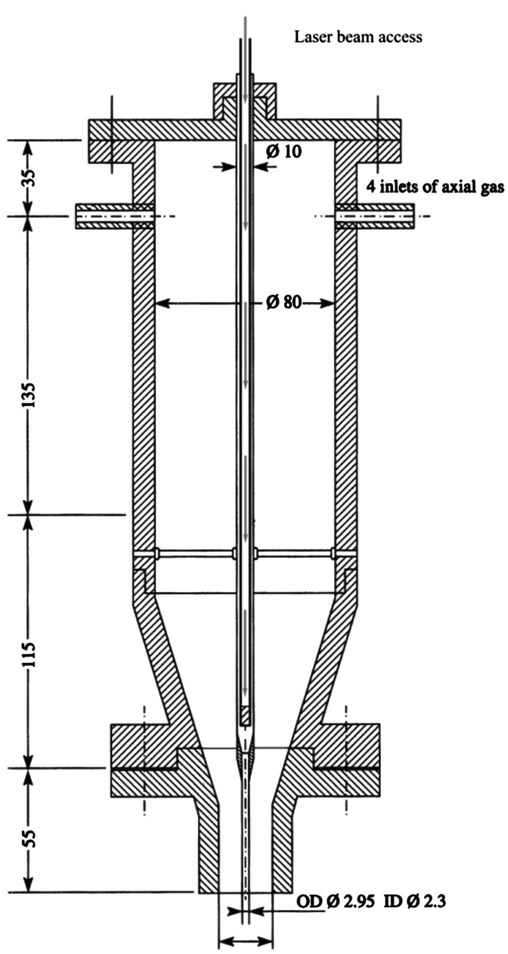

Fig. 1 Geometry of coaxial air-blast atomizer. The path of the laser beam through the laser light-guide tube within the liquid jet is shown by arrows.

It should be noted that, for different types of liquid jet atomizers, the introduction of the beam through a light-guide tube or an optical fiber should be adequate for the implementation of the technique as long as the laser beam enters the liquid stream parallel to the direction of the flow. In this way, it should be possible to propagate along the liquid stream. However, for liquid film atomizers, the introduction of the laser beam to the stream would be more complicated. A possible implementation, in this case, could be the introduction of the laser beam, again by a light-guide tube, only into a part of the liquid film so that only a strip of the liquid film is illuminated. Nevertheless, because this paper presents the first application of the new technique, more testing is required to determine the requirements for the introduction of the laser beam to other atomizer geometries.

The introduction of the laser beam through the liquid jet nozzle is combined with the addition of fluorescing Rhodamine WT dye [20] within the liquid. The addition of the dye results in the emission of fluorescent light from the liquid volume present along the path of the laser beam. Two reasons make the addition of the dye advantageous. The first is that, as the laser beam propagates through the liquid core, it interacts with the surface of the liquid jet and some light may be scattered, leading to difficulties in detecting the interface between the air and the liquid jet. The addition of the dye results in the emission of fluorescing light from the liquid jet core that can be detected at a longer wavelength than that of the incoming laser beam and thus avoid background noise on images due to the scattered light. The second reason is that the fluorescing light is emitted from every where within the liquid jet core and therefore tracks the volume of the liquid, as opposed to the scattered light, which is associated with the interface between the air and the liquid jet. To ensure that the absorption of the incident light remained low along the length of the continuous jet, the concentration of the fluorescing dye was adjusted so that the optical depth of the dye–water solution was greater that 1000 mm (or about 420 liquid jet diameters).

The dye was excited at 532 nm by a pulsed Nd:YAG laser. The energy of each pulse was about 100 mJ and its duration approximately 5 ns. The short duration of the laser pulses allowed the image of the liquid core to be effectively frozen in time. The laser pulses were steered into the light-guide tube by a right angle prism mounted on an adjustable base. To make full use of the pulse energy, the beam diameter was reduced by a system of lenses in Galilean configuration, so that the entire laser light can propagate through the light-guide tube.

In addition to the internal illumination of the liquid jet with the laser, the spray was also back illuminated by a nanosecond xenon flash lamp for shadowgraphic imaging of the liquid core, which is used for comparison with the laser-induced fluorescence (LIF) images. The duration of the flash lamp pulse (80 ns half-width duration), although longer than that of the laser pulse, was short enough to ensure instantaneous imaging. Because the emission spectrum of the fluorescing dye and the emission spectrum of the xenon flash lamp overlap significantly, separation of the two by means of optical filters would cause a considerable loss of signal intensity on the images. Instead, it was preferred that the laser and flash lamp pulses be temporally separated by 2 μs. This ensured complete separation of the two light pulses, although the time delay is short relative to the time scales of the considered flows for any significant change of the flow to occur.

The imaging system comprised two intensified 16-bit charge-coupled device cameras, one for imaging the fluorescent light emitted from the continuous liquid jet core and one for imaging the shadowgraphs of the spray. The camera used for imaging the fluorescent emission from the continuous core was also fitted with a long pass filter to suppress the scattered light from the laser beam. Both cameras were gated for 2 μs to ensure that background optical noise remained minimal.

When considering the effect of the flow conditions at the nozzle on the atomization of the injected liquid, two scaling approaches are generally used. One approach (Eroglu et al. [21]) describes the flow conditions in terms of the liquid Reynolds number:

$$Re_L = \frac{U_L D_L}{\nu_L} \tag{1}$$

and the aerodynamic Weber number:

$$We = \frac{\rho_G (U_G - U_L)^2 D_L}{\sigma} \tag{2}$$

This approach has received acceptance. However, Engelbert et al. [11] have shown that a scaling approach based on the gas to liquid momentum ratio:

$$MR = \frac{\rho_G U_G^2 (D_G^2 - D_0^2)}{\rho_L U_L^2 D_L^2} \tag{3}$$

can describe better the breakup process and the resulting stable droplets over a wide range of operating conditions. This scaling approach was followed by Lasheras et al. [8] to characterize their spray characteristics. Here, both approaches are considered.

Measurements of the liquid jet were initially obtained for a jet in a quiescent air environment, so that the ability of the liquid jet core to act as an optical fiber and transmit the laser light could be evaluated. Four liquid jet velocities were considered, which are summarized in Table 1.

Following the measurements with injection in a quiescent environment, measurements were obtained for liquid jets in a coaxial airstream. The flow conditions at which measurements were obtained are summarized in Table 2. Three liquid flow rates were considered and, for each liquid flow rate, the air flow rate was progressively increased. All measurements were obtained at room temperature and pressure. For each case, 1000 images were recorded.

III. Results and Discussion

The experimental investigation was divided in two parts. In the initial part, the potential of the liquid jet core to act as an optical fiber and transmit laser light along the volume of the liquid jet was investigated and the liquid jet was injected in quiescent air (breakup did not take place within the imaged area). The jet velocity was progressively increased, resulting in an increase of the surface roughness on the liquid jet. Images of the fluorescing jet core as well as diagrams of the fluorescent intensity along the jet core axis are presented and the light penetration within the liquid jet is discussed.

In the second part, the fluorescence technique was implemented in coaxial air-blast atomization for the test conditions of Table 2. Characteristic images of the jet core acquired simultaneously with shadowgraphy and internal illumination of the liquid core are presented for all test conditions. The breakup length of the liquid jet was calculated from both techniques and comparison is presented between the two techniques as a function of We, Re_L, and MR.

Table 1 Considered flow conditions for measurements with injection in a quiescent environment

U_L, m/s	Re_L
1.2	3265
2.0	5442
4.0	10,854
8.0	21,769

Table 2 Considered flow conditions for air-blast atomization measurements

Flow	U_G, m/s	U_L, m/s	We	Re_L	MR
1a	47	2	80	5442	27.4
1b	70	2	185	5442	61.7
1c	119	2	526	5442	171.3
1d	166	2	1041	5442	335.7
2a	47	4	73	10,854	6.9
2b	70	4	175	10,854	15.5
2c	119	4	508	10,854	43.1
2d	166	4	1016	10,854	84.4
3a	47	8	60	21,769	1.7
3b	70	8	154	21,769	3.9
3c	119	8	473	21,769	10.7
3d	166	8	966	21,769	21.0

A. Injection in Quiescent Air

The ability of the continuous core of the liquid jet to transmit the laser light was evaluated by obtaining fluorescent intensity images of the jet core for injection of liquid with jet average velocities indicated in Table 1. To ensure that the fluorescent intensity along the liquid jet length is not attenuated due to absorption by the dye, the concentration of the dye was maintained low enough so that the optical depth of the liquid jet was much longer than the length of the imaged area, as explained in the previous section.

For the considered injection velocities of the liquid jet of this investigation, it was observed that, as the velocity of the liquid jet increased, the surface roughness of the liquid jet also increased. As a result, a more profound decrease of the fluorescent intensity along the jet length was observed at the higher injection velocities, which can be attributed to the increase of the light scattering losses at the jet surface. This is demonstrated in Fig. 2. In Fig. 2a, it can be seen that, for the injection velocity of $U_L = 2$ m/s, where the jet surface is smooth, the attenuation along the continuous core is low as the fluorescent intensity does not decrease considerably along the length of the jet. Conversely, for the maximum jet velocity of $U_L = 8$ m/s, where the surface of the liquid jet changes from smooth to wavy (Fig. 2b), considerable loss of fluorescent intensity can be observed along the liquid jet axis. This is because the increased amount of features along the jet surface causes the angle of incidence between the laser light rays and the liquid surface to be less than the critical angle for total reflection (49 deg for water in air) and, as a result, the scattering of the laser light due to refraction through the surface of the liquid jet is increased. Despite the difference in the mean fluorescent intensity profile, a common feature in both images is the existence of bright spots along the liquid jet. We believe that these are the result of the focusing of the laser beam within the liquid jet from surface features that act as minute mirrors. These bright areas could identify locations along the surface of the continuous jet core where there are significant changes of the surface structure.

Looking at the profiles of the fluorescent intensity for $U_L = 1.2$ m/s (Fig. 3a), there is very little attenuation along the jet length; in the case of $U_L = 2$ m/s (Fig. 3b), there is a decrease of intensity from the nozzle exit to the end of the liquid jet core of about 15%, which results in an optical depth of about 130 liquid jet diameters. It should be noted that the first intensity maximum signifies the location of the nozzle tip and is due to the deposition of dye from the atomizing liquid at the nozzle exit. For $U_L = 4$ m/s (Fig. 3c), the decrease of intensity reached 30% (optical depth about 50 liquid diameters) and, for the maximum liquid velocity (Fig. 3d), the intensity losses were about 70% (optical depth about 15 liquid diameters). As explained earlier, this energy loss is due to incident laser light scattered due to refraction at the liquid–air interface, which has more wavy features as the liquid velocity increases. Although the energy losses are substantial for high U_L, for all cases, the laser light pulse was able to propagate through the entire length of the visualized region of the liquid jet. As a consequence, the observed attenuation is expected to be less in the coaxial air-blast atomizer, because the breakup length will be shorter than the attenuation length when the air flow is present. It should be emphasized that the proposed technique is beneficial when the atomization occurs close to the nozzle and droplets exist around the liquid jet core. Otherwise, simple photography would be adequate to measure the breakup length.

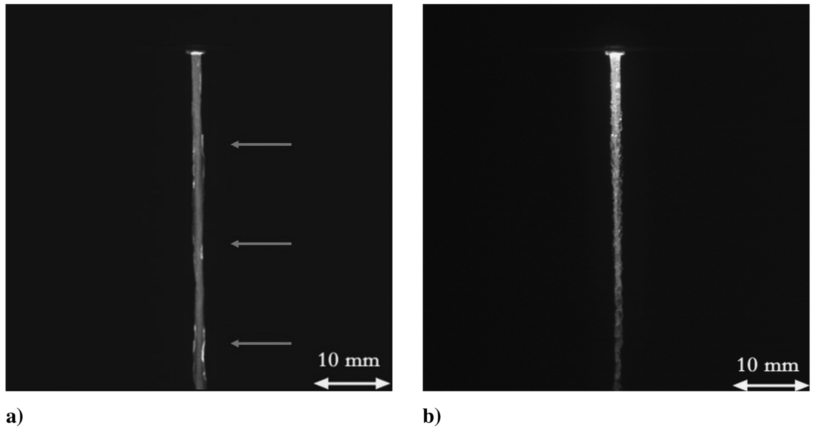

Fig. 2 Fluorescent images of a liquid jet injected in quiescent air at a) $U_L = 2$ m/s (minor decrease of the fluorescent intensity along jet length, bright spots appear at regular intervals marked with arrows), and b) $U_L = 8$ m/s (significant decrease of the fluorescent intensity along jet length, no regular patterns).

It can also be observed from the intensity profiles for $U_L = 1.2$ m/s (Fig. 3a) and $U_L = 2$ m/s (Fig. 3b) the occurrence at regular spatial intervals of about 10 and 15 mm, respectively, of local maxima of fluorescent intensity along the jet axis. This is due to the presence of the bright areas along the liquid jet, which were identified in Fig. 2a, and was verified that they are not due to noise by the uniform background of the intensity distribution along the jet axis. The presence of these areas at the specific locations along the jet core supports the proposal that they are manifestations of surface features, which cannot clearly be distinguished by plain shadowgraphy but are shown with the LIF technique to appear at regular intervals and with a spatial frequency that is decreasing with liquid flow rate. It is also interesting to observe that, in the regions of interest, the local maximum intensity and its spatial spread increase with distance from the

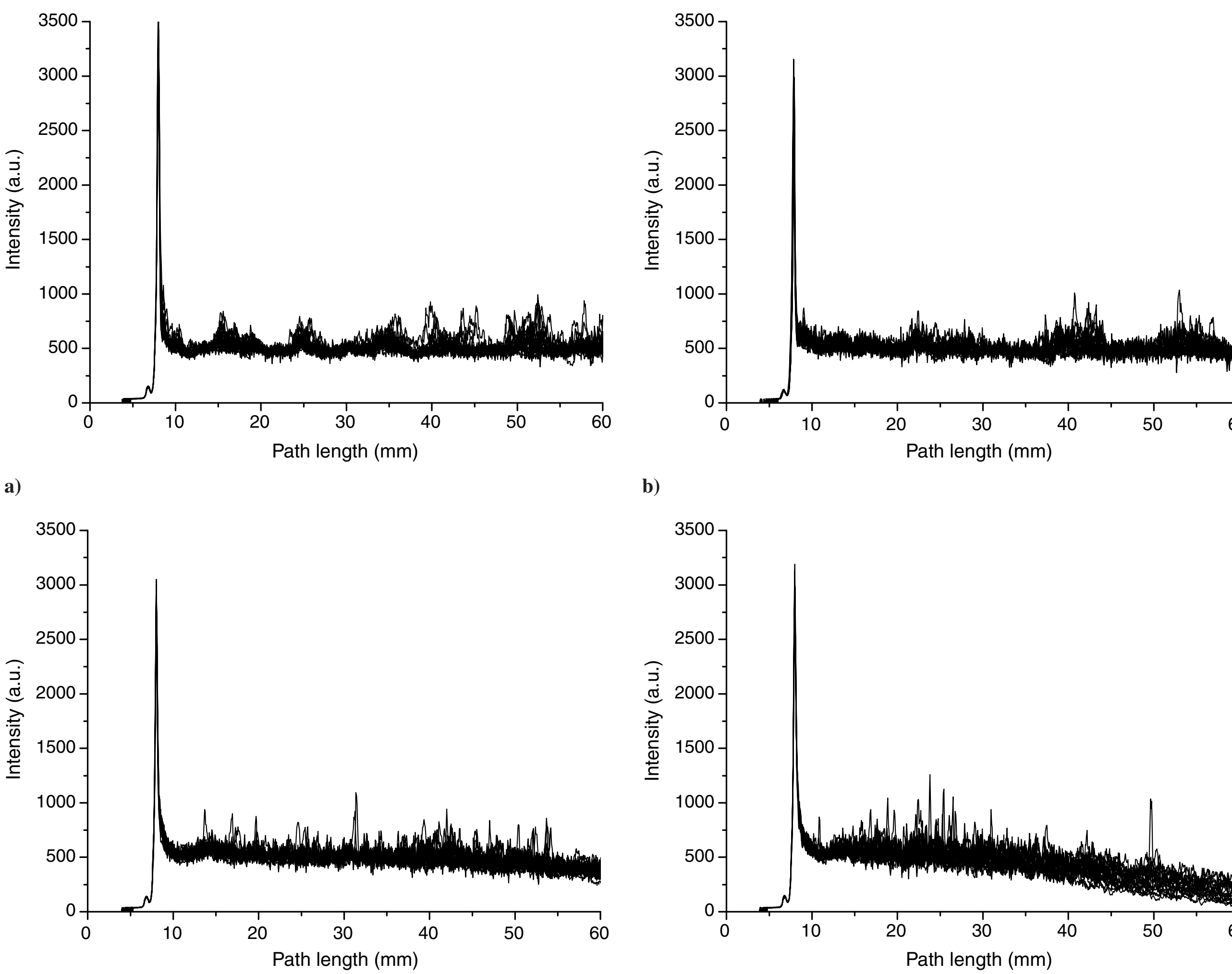

Fig. 3 Fluorescent intensity variation along the axis of the liquid jet for injection in a quiescent environment. Fluorescent intensity is averaged across the local jet diameter; results for cross section averaged liquid velocity at the nozzle exit of a) $U_L = 1.2$ m/s, b) $U_L = 2$ m/s, c) $U_L = 4$ m/s, and d) $U_L = 8$ m/s.

nozzle exit, which indicates that more surface features are growing along the jet length.

For $U_L = 4$ m/s and $U_L = 8$ m/s (Figs. 3c and 3d, respectively), the intensity maxima cannot be observed at constant locations along the jet path, but rather intensity maxima appear throughout the whole jet length. From this, it can be inferred that, as the liquid velocity increases and the liquid flow becomes more turbulent, the location of the wavy features on the surface becomes random.

B. Air-Blast Atomization

1. Phenomenological Interpretation

With the introduction of the air coflow, atomization and breakup of the jet core take place close to the nozzle exit. Characteristic sample images acquired for each test condition are presented for the fluorescence technique along with their simultaneous shadowgraphic equivalent (Figs. 4–6).

For the lowest jet velocity ($U_L = 2$ m/s) and for the lowest air coflow conditions ($U_G = 47$ m/s and $U_G = 70$ m/s), where the shadowgraph is not obstructed by droplets, there is generally agreement between the two techniques (as shown in Figs. 4a–4d) albeit with a decrease in the fluorescent intensity before the breakup point, probably due to laser light intensity losses at the air–liquid interface due to the reduction of the liquid jet diameter. However, it is not easy to determine in an objective way the exact location of the liquid jet breakup from shadowgraphs.

As the gas velocity increases ($U_G = 119$ m/s and $U_G =$ 166 m/s) and the atomization becomes more vigorous, the breaking point of the jet core is partially obstructed in the shadowgraphic images (Figs. 4e and 4g). The fluorescent intensity images of the continuous liquid core do not have the same problem (Figs. 4f and 4h) and the laser light can trace well the air–liquid interface. A decrease of the sharpness of the fluorescence image close to the breakup point can be attributed to the roughened surface of the jet due to droplet detachment and the surrounding droplets. Therefore, the improved ability of the novel fluorescence technique to measure the breakup length of the liquid jet objectively is demonstrated.

As the liquid jet velocity increases ($U_L = 4$ m/s), the flow inside the liquid jet core becomes more turbulent and the continuous jet core length increases. For the two lower gas velocities ($U_G = 47$ m/s and $U_G = 70$ m/s), the breakup region is generally free of obstruction from surrounding ligaments (Figs. 5a–5d). Similar to the previous case for the same gas velocities, there is agreement between the two techniques, albeit with the LIF technique showing somewhat shorter lengths. When increasing the gas velocity to $U_G = 119$ m/s, there is a discrepancy between the two techniques. For example, in the sample images presented, the breakup length from the shadowgraph (Fig. 5e) appears to be extending below the middle of the image, which is longer that the breakup length of Fig. 5c, which corresponded to flow conditions of the same U_L and lower U_G, and this trend is erroneous. The simultaneous fluorescent intensity image (Fig. 5f), on the other hand, reveals a shorter length, which is according to expectations. For the maximum air velocity ($U_G = 166$ m/s), there is still disagreement, but the discrepancy is not large. As before, the shadowgraph of the jet core does not identify clearly the breakup location due to the existence of surrounding droplets. Therefore, the LIF technique is more accurate for flows leading to shorter breakup lengths and dense sprays.

At the maximum liquid velocity ($U_L = 8$ m/s), the shadowgraphs (Figs. 6a and 6c) of the atomizing jet show that the continuous core length extends beyond the imaged area for the lower gas velocities ($U_G = 47$ m/s and $U_G = 70$ m/s). The fluorescent image of the jet core, on the other hand, shows that for $U_G = 47$ m/s (Fig. 6b) the jet is continuous up to the end of the imaged area, whereas for $U_G =$ 70 m/s (Fig. 6d), it shows that the breakup has occurred within the imaged area. It is difficult to decide whether it is the shadowgraphic or the LIF images that depict the continuous core correctly. However, the three-dimensional structure of the liquid jet may give the wrong impression for the breakup length with the shadowgraphic technique, whereas the fluorescence technique should indicate an interruption of light propagation through the liquid when a discontinuity occurs. For the higher air velocities ($U_G = 119$ m/s and $U_G = 166$ m/s), presented in Figs. 6e–6h, the shadowgraphs are ambiguous as the products of atomization that hinder the imaging of the liquid core, whereas the LIF technique indicates a shorter breakup length than the implied length from the shadowgraphs. As the air velocity increases, breakup is expected to occur closer to the nozzle and this trend is indicated by the LIF technique, whereas shadowgraphy is difficult to interpret. However, the details of light propagation within the liquid jet at regions where the liquid jet becomes very thin must be examined to evaluate the uncertainty of the LIF technique.

From the comparison of LIF and shadowgraphic images, it can be seen that the LIF technique has advantages, as droplets and ligaments along the imaging path do not obstruct the LIF measurement of the breakup length significantly. As a consequence, it can provide an objective measurement that is independent of the interpretation of the images by the user. The latter is not true for the shadowgraphic images, when the flow conditions lead to good atomization and therefore dense sprays in the near nozzle region.

Nevertheless, there are three effects that could cause some difficulties with the LIF technique. The first is scattering losses of the propagating light beam along the jet core, due to the structures at the liquid jet surface, as demonstrated previously for injection in quiescent air. When the jet is atomizing, the surface of the core becomes rougher than in the case of injection in quiescent air and therefore the scattering losses at the air–liquid interface are increasing. This is demonstrated in Fig. 7, where the scattered light coming from the surface of a jet of $U_L = 4$ m/s that is injected in quiescent air (Fig. 7a) is compared with the scattered light coming from the same jet with the introduction of a coflow of air of $U_G =$ 70 m/s (Fig. 7b). It can be observed that the scattering losses along the length of the continuous liquid jet increase, due to the air coflow and the laser beam, will not be able to propagate for a great distance along the jet length. Nevertheless, the scattered light signal is minimal close to the base of the liquid jet and only becomes significant away from the liquid jet nozzle exit where the atomization is more rigorous. As such, the greatest loss of the laser light intensity (and consequently of the fluorescent signal intensity) occurs close to the breakup point. Therefore, the light intensity close to the breakup point should be sufficient for the identification of the breakup location. Additionally, a comparison between the scattered light image of the liquid jet core (Fig. 7b) with the simultaneously recorded LIF image of the core (Fig. 7c) for the same flow conditions ($U_L = 4$ m/s and $U_G = 70$ m/s in this example) shows that the breakup length of the LIF intensity is shorter than the scattered light signal. This suggests that the continuity of the jet core is broken and the LIF signal diminishes, as expected, because it is produced mainly from the volume of the continuous core. However, the scattered light signal can persist a little further downstream due to defusing of the laser light at the surface of the produced droplets and ligaments downstream of the breakup region. Therefore, the LIF technique is expected to measure accurately the breakup length.

The second effect that causes some uncertainty in the technique occurs at locations where there is a narrowing of the liquid jet due to the high amplitude of the wavy structures that develop along the surface to form constrictions on the jet core. The effect of such constrictions is twofold. One is that, at these locations, there is a considerable amount of the laser beam power lost to scattering, but perhaps more important is that the light that does propagate through the constriction is largely reduced in diameter and is not always able to expand to illuminate the whole volume of the jet downstream of the constriction. Thus, visualization of the jet core downstream is limited. This effect can be better understood if seen exemplified in Fig. 7 for a dripping flow. After the constriction, the laser light clearly follows a straight path without being able to illuminate the whole volume of liquid downstream the constriction (Fig. 7d). It is not possible to compensate for the effect of the local narrowing of the jet diameter as it is due to the shape of the atomizing liquid jet. Therefore, it is possible that, depending on the geometry of the liquid jet, systematically shorter values of the breakup length are measured in certain flow conditions. However, when there is such a decrease of the cross section of the liquid jet, it is highly likely that the continuity

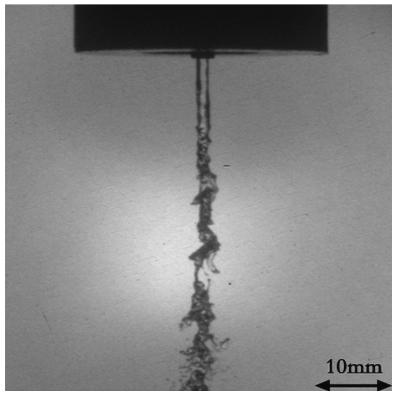

a) Jet shadowgraph at U_L=2.0m/s and U_G=47m/s

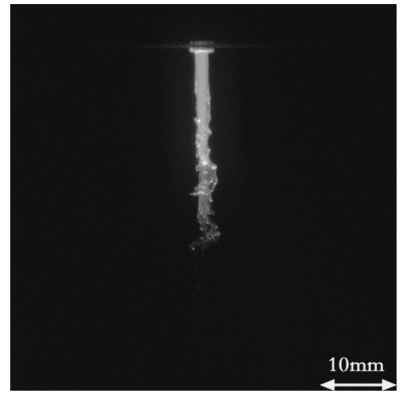

b) Jet LIF image at U_L=2.0m/s and U_G=47m/s

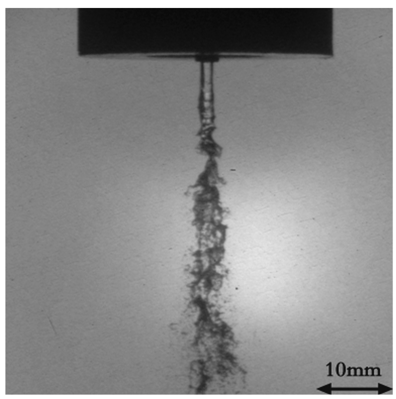

c) Jet shadowgraph at U_L=2.0m/s and U_G=70m/s

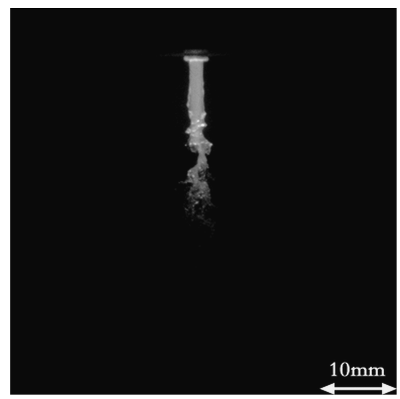

d) Jet LIF image at U_L=2.0m/s and U_G=70m/s

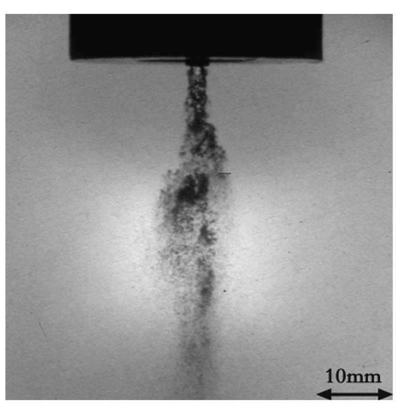

e) Jet shadowgraph at U_L=2.0m/s and U_G=119m/s

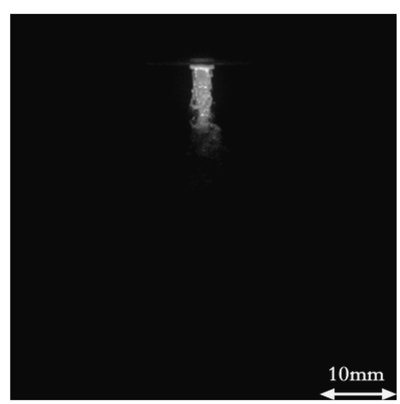

f) Jet LIF image at U_L=2.0m/s and U_G=119m/s

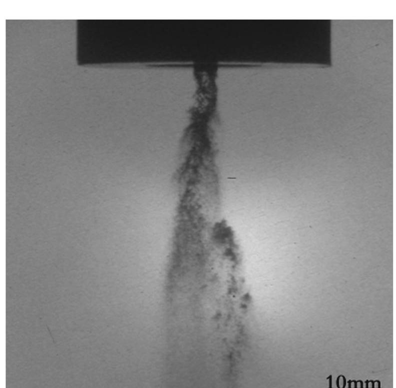

g) Jet shadowgraph at U_L=2.0m/s and U_G=166m/s

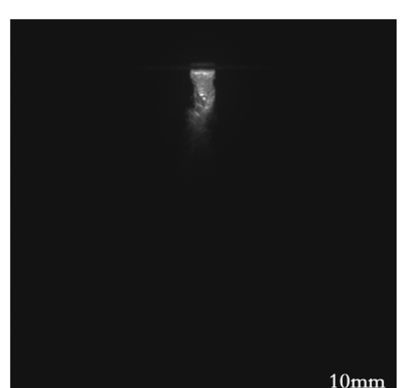

h) Jet LIF image at U_L=2.0m/s and U_G=166m/s

Fig. 4 Comparison between simultaneous shadowgraphy and LIF imaging for cross section averaged liquid velocity $U_L = 20$ m/s and variable coaxial gas velocity.

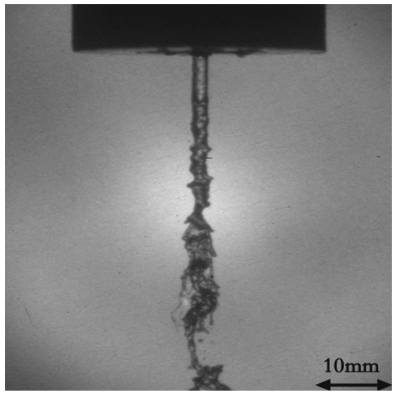

a) Jet shadowgraph at U_L=4.0m/s and U_G=47m/s

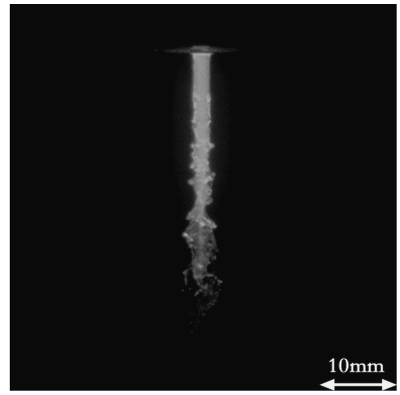

b) Jet LIF image at U_L=4.0m/s and U_G=47m/s

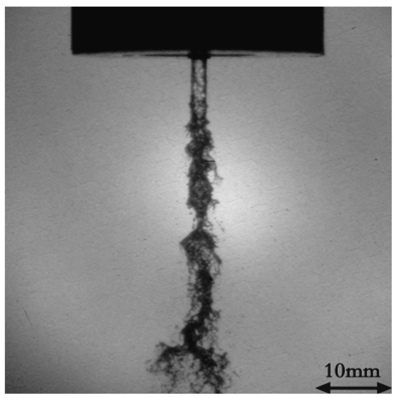

c) Jet shadowgraph at U_L=4.0m/s and U_G=70m/s

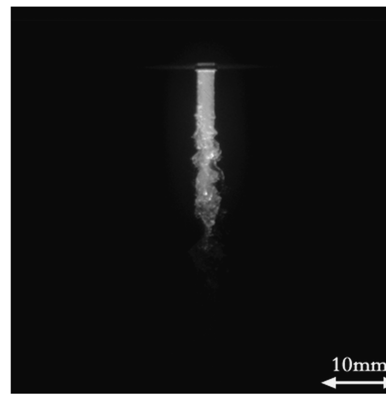

d) Jet LIF image at U_L=4.0m/s and U_G=70m/s

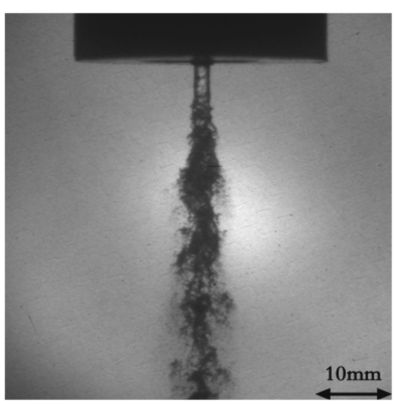

e) Jet shadowgraph U_L=4.0m/s and U_G=119m/s

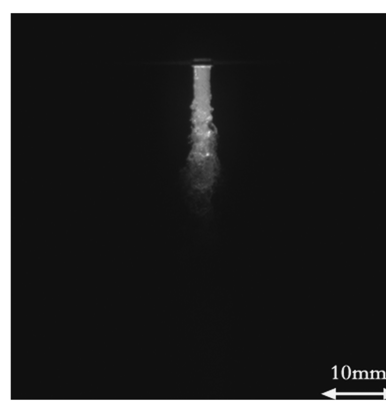

f) Jet LIF image at U_L=4.0m/s and U_G=119m/s

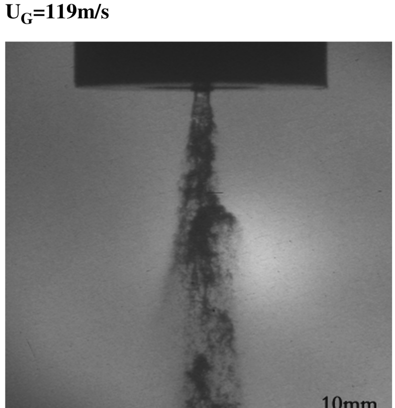

g) Jet shadowgraph U_L=4.0m/s and U_G=166m/s

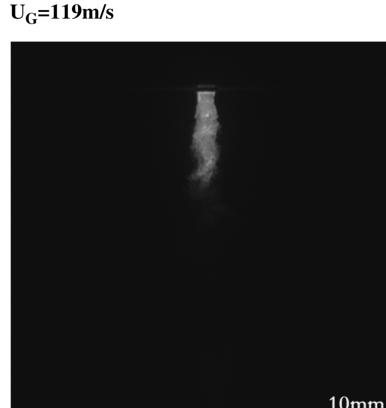

h) Jet LIF image at U_L=4.0m/s and U_G=166m/s

Fig. 5 Comparison between simultaneous shadowgraphy and LIF imaging for cross section averaged liquid velocity $U_L = 4.0$ m/s and variable coaxial gas velocity.

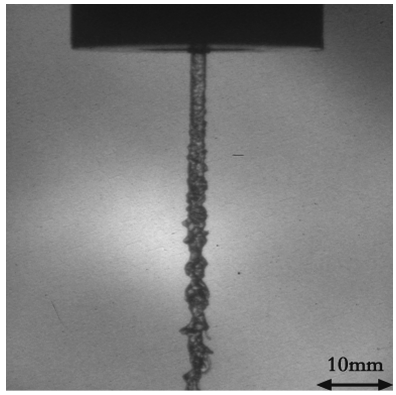

a) Jet shadowgraph at U_L=8.0m/s and U_G=47m/s

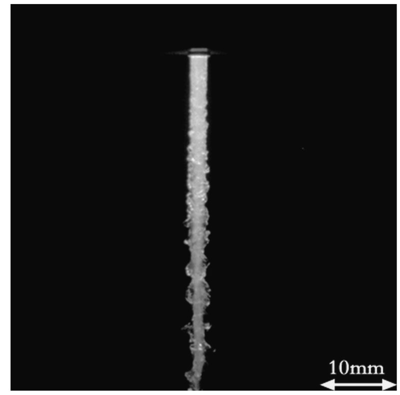

b) Jet LIF image at U_L=8.0m/s and U_G=47m/s

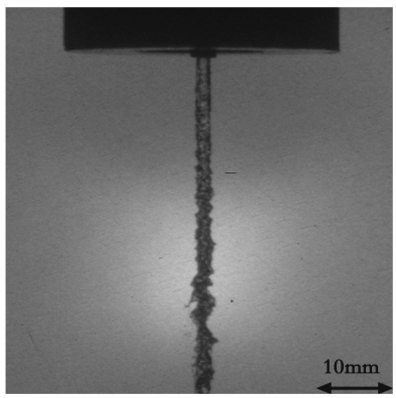

c) Jet shadowgraph at U_L=8.0m/s and U_G=70m/s

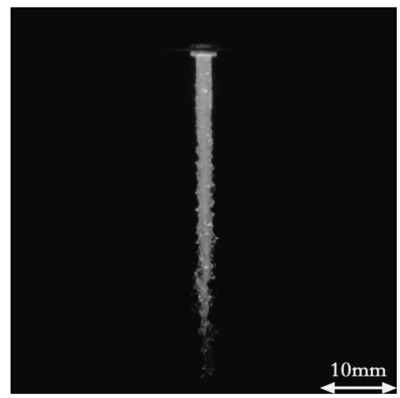

d) Jet LIF image at U_L=8.0m/s and U_G=70m/s

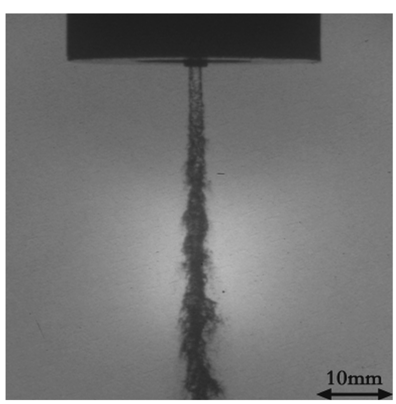

e) Jet shadowgraph at U_L=8.0m/s and U_G=119m/s

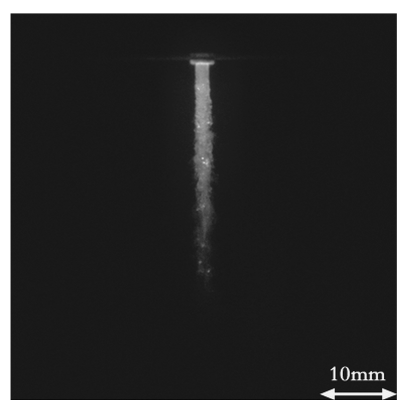

f) Jet LIF image at U_L=8.0m/s and U_G=119m/s

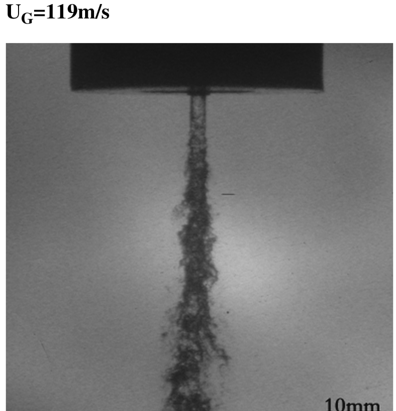

g) Jet shadowgraph at U_L=8.0m/s and U_G=166m/s

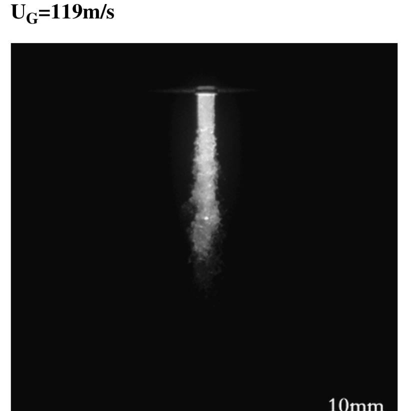

h) Jet LIF image at U_L=8.0m/s and U_G=166m/s

Fig. 6 Comparison between simultaneous shadowgraphy and LIF imaging for cross section averaged liquid velocity $U_L = 8.0$ m/s and variable coaxial gas velocity.

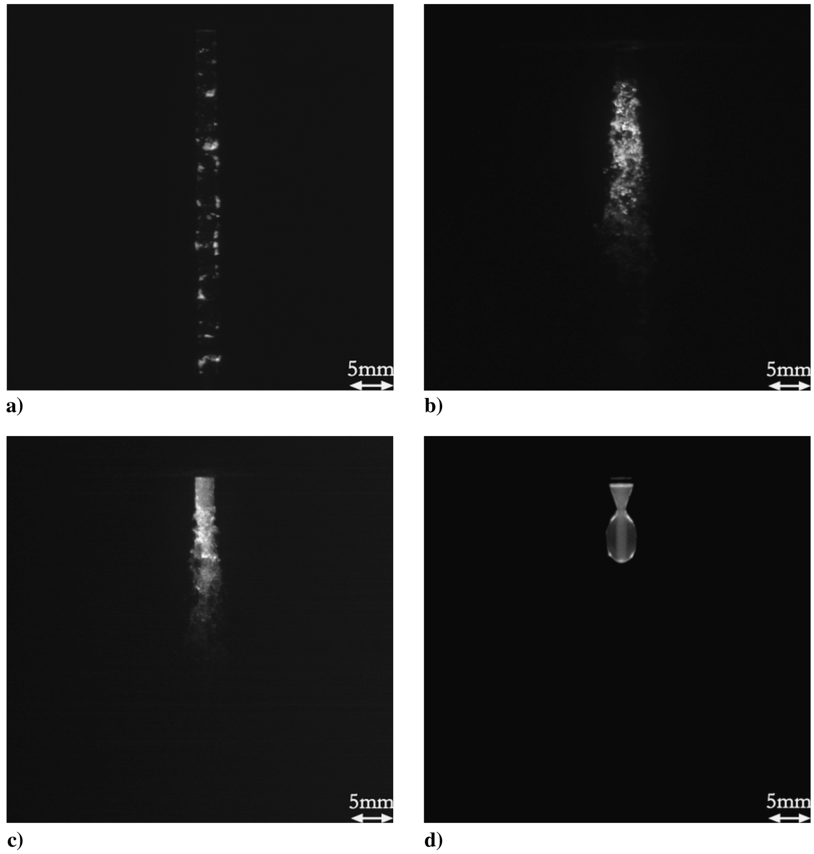

Fig. 7 Examples of scattered and fluorescent intensity images of an internally illuminated jet: a) scattered light from the surface of the liquid jet at $U_L = 4$ m/s and no air coflow, b) scattered light from the surface of the liquid jet at $U_L = 4$ m/s and $U_G = 70$ m/s (flow 2b), c) LIF image from the volume of the liquid jet at $U_L = 4$ m/s and $U_G = 70$ m/s (flow 2b), and d) LIF image of dripping flow showing that the beam is unable to expand after a narrow constriction to fill the whole volume of liquid downstream.

of the jet core will not persist and that breakup will occur close to this narrow region. As a consequence, any systematic bias in the LIF measurement of the breakup length is expected to be small for flows with good atomization.

Finally, when atomization becomes vigorous, the fluorescent light emitted from the jet core is subject to multiple scattering on the surrounding spray droplets leading to some loss of contrast on the liquid jet core images. However, the path through the spray droplets that the fluorescent light emanating from the jet core has to travel is only half the distance that back-illuminated light has to travel for shadowgraphic images. Therefore, the loss of image contrast of the liquid jet in dense sprays is expected to be significantly lower for the fluorescent light of the proposed technique than for the back-illuminated light of shadowgraphy.

2. *Measurement of the Average Breakup Length*

For the evaluation of the breakup length, the profile of the fluorescent intensity along the path of the liquid jet was calculated from each LIF image of the atomizing jet, by averaging the fluorescent intensity across the jet diameter for each distance from the nozzle exit. An example is presented in Fig. 8, where the fluorescent intensity, averaged across the jet diameter, is plotted along the distance from the image top normalized to the liquid nozzle diameter. The first intensity maximum signifies the location of the nozzle tip and is due to the deposition of dye from the atomizing liquid at the nozzle exit. Beyond the tip of the nozzle, the fluorescent intensity decreases downstream the jet axis and, although sporadic intensity maxima do exist, which are due to bright spots along the liquid jet core as mentioned earlier, they do not cause problems in the evaluation of the breakup length. To measure the breakup length, the fluorescent intensity is tracked down from the jet nozzle to the point along the jet length where its value drops below a certain threshold. The value of the threshold was chosen to be 20% of the fluorescent intensity of the jet core after the nozzle exit. This value was selected because, close to the breakup point where there is a fast decrease of the fluorescence intensity (increased scattering losses close to the breaking point) which is followed by a reduction of the remaining signal at a lower rate (some fluorescence is diffused on the products of atomization), the intensity of the fluorescence signal is about 20% of the intensity at the base of the nozzle. However, the value of 20% is not an absolute criterion and it is possible that at the breaking point of the jet the fluorescent intensity is somewhat different. However, the choice of the threshold value of 20% was satisfactory, because moderate changes of the threshold will lead to small changes of the measured value of the breakup length. Additionally, the setting of the condition of breakup as a fraction of the fluorescent intensity at the base of the atomizing jet has the benefit that each image contains all the information required for the estimation of the breakup length. Therefore, independent calibration is not required and the technique

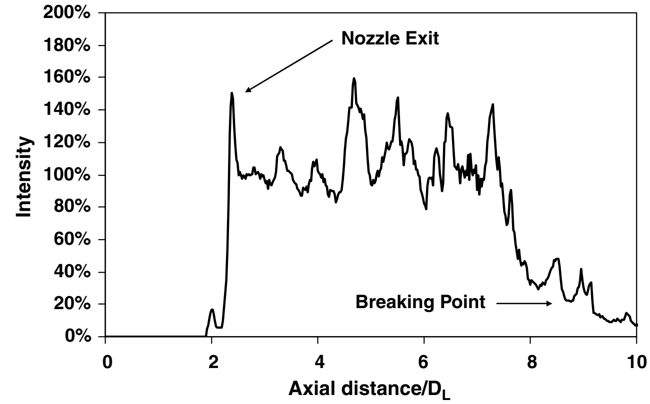

Fig. 8 Example of fluorescent intensity change along the axis of the atomizing jet.

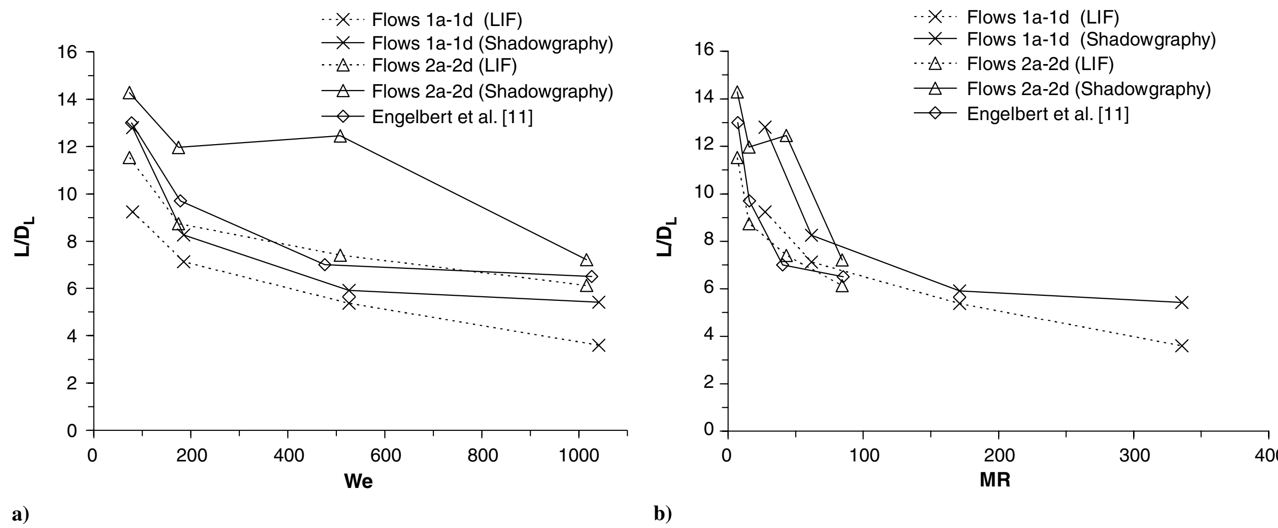

Fig. 9 Comparison of variation of time-averaged breakup length with a) Weber number *We* and b) momentum ratio *MR*, as measured by the shadowgraphic and the novel LIF techniques.

is not sensitive to the absolute intensity of the laser. Nevertheless, the laser pulse energy should be sufficiently high for the intensity along the jet core to be significantly higher than the background signal. To avoid errors, from the sporadic intensity maxima or minima, the fluorescent intensity profile was smoothed by averaging the fluorescent intensity along a number of pixels (corresponding to about 0.2 nozzle diameters) in the direction of the jet axis.

The measurement of the breakup length from the acquired images was performed only for conditions $U_L = 2$ m/s and $U_L = 4$ m/s, because at $U_L = 8$ m/s the light losses might interfere with the accuracy of the technique. The measured values of the breakup length from the internal illumination technique and the shadowgraphic technique are presented in Fig. 9, normalized by the inner diameter of the liquid jet D_L and plotted against the We number (Fig. 9a) and the MR (Fig. 9b). In addition to the measurements of this study, the values obtained by Engelbert et al. [11] on the same atomizer are presented for comparison.

The breakup length is reduced with the increase of We number (Fig. 9a), for the two considered Re_L, and both shadowgraphy and the novel LIF technique measure a similar trend. However, it can be observed that, for all values of We, the breakup length measured by the LIF technique is consistently lower than the values obtained by the shadowgraphic technique, as expected from the comparison of the instantaneous images presented earlier. As discussed before, this is due to the existence of products of atomization that make the breakup length appear longer than it actually is in the shadowgraphs. This is especially true for the higher air velocities, where atomization is more vigorous (see, for example, sprays for flows 1d and 2c, where the difference of the breakup length measured by the two techniques can reach up to 40%). However, for flows 1c and 2d, the difference is only on the order of 15%. For such flows, the length of the atomizing jet is short and will not become highly constricted or contorted before breakup. Therefore scattering losses are not considered to have a key effect in the evaluation of the length of the liquid jet with the LIF technique, whereas the obstruction of the shadowgraphs by the products of atomization is significant. The scattering losses close to the breakup region have an influence on the accuracy of the evaluation of longer breakup lengths where the difference between the two methods is up to 30%. As pointed out earlier, for conditions where the connectivity between subsequent volumes of liquid is small, as it is frequently in these flows, the proposed technique will identify such points as discontinuous. Nevertheless, the LIF technique is intended to be used for conditions with good atomization, where the sprays are dense and the shadowgraphic approach fails.

The breakup length as a function of MR is presented in Fig. 9b. As suggested by Engelbert et al. [11], it can be seen that the values of the breakup length follow, approximately, a single trend regardless of Re_L. The difference between shadowgraphy and LIF technique increases with MR. This is because, although the presence of the products of atomization make the shadowgraphic images more difficult to interpret, the LIF technique could more successfully illuminate the liquid core as it became shorter at higher MR.

A point of significant discrepancy between the two techniques appears for flow 2c where there is an overprediction of the breakup length from the shadowgraphic technique. This is due to the obstruction of the shadowgraphs by the products of the jet breakup, which do not allow the clear imaging of the jet core with back illumination. In contrast, the LIF technique is not affected by these obstructions (except perhaps in a decrease of the image contrast) and this is where the proposed technique is shown to have a clear advantage.

Finally, it can be seen that there is good agreement between the results of Engelbert et al. [11] and current measurements, as the values of the breakup length measured in that study agree well with the breakup length of this investigation that was obtained with the LIF technique and are shorter that the breakup length values measured with shadowgraphy. The lack of overestimation of the breakup length around $We = 500$ in the study of Engelbert et al. [11] is noticeable. A possible explanation could be that their measurements were time resolved and it was easier to decide the breaking point of the liquid jet from the temporal sequence of the breakup process, which gives support to the hypothesis that the jet continuity is likely to break at locations where the jet becomes thin.

IV. Conclusions

A novel optical method has been proposed for the measurement of breakup length of liquid jets in atomizers based on laser light illumination of the liquid jet through the nozzle. The continuous core of the liquid jet is visualized by means of laser-induced fluorescence, produced by excitation of a dye present in the liquid. The approach relies on the liquid jet acting as an optical fiber, which transmits the laser light until it is interrupted when the liquid jet breaks up.

The novel technique was tested on sprays produced by an air-blast atomizer operating with and without coaxial air flow and the results were compared with simultaneous shadowgraphic measurements. The investigation has shown that the proposed technique is able to measure at conditions where shadowgraphy is obstructed by the products of atomization, which are present around the liquid jet. The values of the breakup length measured by the LIF technique are systematically shorter than the values obtained with shadowgraphy for all flow conditions. These results generate reservations on the precision of existing empirical correlations for the breakup length, which are mainly based on shadowgraphic measurements.

Although it has been shown that the proposed LIF technique has limitations for operating conditions when the liquid jet continuous core is long due to laser light attenuation caused by scattering at the air–liquid interface, these limitations are alleviated when the continuous core becomes shorter. However, the proposed LIF technique is to be used for flow conditions leading to shorter breakup lengths, which are associated with good atomization and dense sprays where shadowgraphy is inaccurate and dependant on the user interpretation of images for dense sprays. However, time-dependent shadowgraphic measurements may be able to remove some of the uncertainty due to the consideration of the temporal behavior of the breakup process assisting the identification of the breakup region.

An additional potential use of the technique was identified from the presence of localized maxima at the integrated LIF intensity along the liquid jet. This characteristic can be used as a marker of wavy structures along the liquid jet surface and, in this way, quantify the wavelength of the associated instabilities of the liquid–air interface.

References

[1] Castleman R. A, "The Mechanism of the Atomization of Liquids," *Journal of Research of the National Bureau of Standards*, Vol. 6, 1931, pp. 369–376.

[2] Lefebvre, A. H., *Atomization and Sprays*, Hemisphere, New York, 1989.

[3] Eroglu, H., and Chigier, N., "Initial Drop Size and Velocity Distributions for Airblast Coaxial Atomizers," *Journal of Fluids Engineering*, Vol. 113, No. 3, 1991, pp. 453–459. doi:10.1115/1.2909517

[4] Hardalupas, Y., and Whitelaw, J. H., "Characteristics of Sprays Produced by Coaxial Airblast Atomizers," *Journal of Propulsion and Power*, Vol. 10, No. 4, 1994, pp. 453–460. doi:10.2514/3.23795

[5] Lasheras, J. C., and Hopfinger, E. J., "Liquid Jet Instability and Atomization in a Coaxial Gas Stream," *Annual Review of Fluid Mechanics*, Vol. 32, Jan. 2000, pp. 275–308. doi:10.1146/annurev.fluid.32.1.275

[6] Varga, C. M., Lasheras, J. C., and Hopfinger, E. J., "Initial Breakup of a Small-Diameter Liquid Jet by a High-Speed Gas Stream," *Journal of Fluid Mechanics*, Vol. 497, 2003, pp. 405–434. doi:10.1017/S0022112003006724

[7] Mayer, W. O. H., and Branam, R., "Atomization Characteristics on the surface of a Round Liquid Jet," *Experiments in Fluids*, Vol. 36, No. 4, 2004, pp. 528–539. doi:10.1007/s00348-003-0675-0

[8] Lasheras, J. C., Villermaux, E., and Hopfinger, E. J., "Breakup and Atomization of a Round Water Jet by a High-Speed Annular Air Jet," *Journal of Fluid Mechanics*, Vol. 357, Feb. 1998, pp. 351–379. doi:10.1017/S0022112097008070

[9] Chehroudi, B., Chen, S. H., and Bracco, F. V., "On the Intact Core of Full-Cone Sprays," Society of Automotive Engineers Technical Paper 850126, 1985.

[10] Yule, A. J., and Salters, D. G., "A Conductivity Probe Technique for Investigating the Breakup of Diesel Sprays," *Atomization and Sprays*, Vol. 4, No. 1, 1994, pp. 41–63.

[11] Engelbert, C., Hardalupas, Y., and Whitelaw, J. H., "Breakup Phenomena in Coaxial Airblast Atomizers," *Proceedings of the Royal Society of London, Series A: Mathematical and Physical Sciences*, Vol. 451, No. 1941, 1995, pp. 189–229. doi:10.1098/rspa.1995.0123

[12] Cai, W. Y., Powell, C. F., Yue, Y., Narayanan, S., Wang, J., Tate, M. W., Renzi, M. J., Ercan, A., Fontes, E., and Gruner, S. M., "Quantitative Analysis of Highly Transient Fuel Sprays by Time-Resolved X-Radiography," *Applied Physics Letters*, Vol. 83, No. 8, 2003, pp. 1671–1673. doi:10.1063/1.1604161

[13] Renzi, M. J., Tate, M. W., Ercan, A., Gruner, S. M., Fontes, E., Powell, C. F., MacPhee, A. G., Narayanan, S., Wang, J., Yue, Y., and Cuenca, R., "Pixel Array Detectors for Time Resolved Radiography (Invited)," *Review of Scientific Instruments*, Vol. 73, No. 3, 2002, pp. 1621–1624. doi:10.1063/1.1435816

[14] Yue, Y., Powell, C. F., Poola, R., Wang, J., and Schaller, J. K., "Quantitative Measurements of Diesel Fuel Spray Characteristics in the Near-Nozzle Region Using X-Ray Absorption," *Atomization and Sprays*, Vol. 11, No. 4, 2001, pp. 471–490.

[15] Linne, M., Paciaroni, M., Hall, T., and Parker, T., "Ballistic Imaging of the Near Field in a Diesel Spray," *Experiments in Fluids*, Vol. 40, No. 6, 2006, pp. 836–846. doi:10.1007/s00348-006-0122-0

[16] Linne, M. A., Paciaroni, M., Gord, J. R., and Meyer, T. R., "Ballistic Imaging of the Liquid Core for a Steady Jet in Crossflow," *Applied Optics*, Vol. 44, No. 31, 2005, pp. 6627–6634. doi:10.1364/AO.44.006627

[17] Paciaroni, M., Linne, M., Hall, T., Delplanque, J. P., and Parker, T., "Single-Shot Two-Dimensional Ballistic Imaging of the Liquid Core in an Atomizing Spray," *Atomization and Sprays*, Vol. 16, No. 1, 2006, pp. 51–69. doi:10.1615/AtomizSpr.v16.i1.40

[18] Colladon, D., "On the Reflections of a Ray of Light Inside a Parabolic Liquid Stream," *Comptes rendus hebdomadaires des séances de l'Académie des sciences*, Vol. 15, 1842, pp. 800–802.

[19] Tyndall, J., "On Some Phenomena Connected with the Motion of Liquids," *Proceedings of the Royal Institution of Great Britain*, Vol. 1, 1854, pp. 446–448.

[20] Melton, L. A., and Lipp, C. W., "Criteria for Quantitative PLIF Experiments Using High-Power Lasers," *Experiments in Fluids*, Vol. 35, No. 4, 2003, pp. 310–316. doi:10.1007/s00348-003-0632-y

[21] Eroglu, H., Chigier, N., and Farago, Z., "Coaxial Atomizer Liquid Intact Lengths," *Physics of Fluids, A: Fluid Dynamics*, Vol. 3, No. 2, 1991, pp. 303–308. doi:10.1063/1.858139

E. Gutmark
Associate Editor